

**Two-neutron removal cross sections from  $^{15,16}\text{C}$  at around 240 MeV/nucleon**

Y. Z. Sun,<sup>1,2</sup> S. T. Wang,<sup>1,\*</sup> Z. Y. Sun,<sup>1</sup> X. H. Zhang,<sup>1</sup> D. Yan,<sup>1</sup> B. H. Sun,<sup>3</sup> J. W. Zhao,<sup>3</sup> Y. P. Xu,<sup>3</sup> D. Y. Pang,<sup>3</sup> Y. H. Yu,<sup>1</sup>  
 K. Yue,<sup>1</sup> S. W. Tang,<sup>1</sup> C. Dong,<sup>1,4</sup> Y. X. Zhao,<sup>1,2</sup> F. Fang,<sup>1</sup> Y. Sun,<sup>1,2,4</sup> Z. H. Cheng,<sup>1,4</sup>  
 X. M. Liu,<sup>1</sup> P. Ma,<sup>1</sup> H. R. Yang,<sup>1</sup> C. G. Lu,<sup>1</sup> and L. M. Duan<sup>1</sup>

<sup>1</sup>CAS Key Laboratory of High Precision Nuclear Spectroscopy, Institute of Modern Physics,  
 Chinese Academy of Sciences, Lanzhou 730000, China

<sup>2</sup>University of Chinese Academy of Sciences, Beijing 100049, China

<sup>3</sup>School of Physics and Nuclear Energy Engineering, Beihang University, Beijing 100191, China

<sup>4</sup>Lanzhou University, Lanzhou 730000, China



(Received 15 November 2018; published 1 February 2019)

The cross sections for two-neutron removal from  $^{15,16}\text{C}$  on a carbon target have been measured at around 240 MeV/nucleon. The measured cross section for  $^{15}\text{C}$  is smaller than for  $^{16}\text{C}$ . The trends of the cross sections for  $^{15,16}\text{C}$  are inconsistent with the previously reported experimental data, but in agreement with the theoretical predictions based on eikonal-model calculations. Based on the present results of  $^{15,16}\text{C}$  combined with the available experimental data on  $^{17-20}\text{C}$ , an odd-even staggering of the two-neutron removal cross sections along the neutron-rich carbon isotopic chain from  $^{15}\text{C}$  to  $^{20}\text{C}$  is observed, and this feature is well reproduced by the theoretical calculations.

DOI: [10.1103/PhysRevC.99.024605](https://doi.org/10.1103/PhysRevC.99.024605)

**I. INTRODUCTION**

One-nucleon removal reactions at intermediate and high energies have been developed as an effective direct reaction for probing the structure of nuclei far from stability [1,2]. The removal of two well-bound like nucleons from asymmetric nuclei has also been shown to proceed as a direct reaction [3–6], while in the case of two weakly bound nucleon removal from a mass  $A$  projectile, the reaction mechanism is complicated. The mass  $A-2$  residue can result from two different mechanisms [7,8]: single-step direct removal of a pair of nucleons and one-nucleon knockout to unbound states of the intermediate mass  $A-1$  residue followed by nucleon evaporation.

The carbon isotopes have a long isotopic chain and the experimental two-neutron removal data for most neutron-rich carbon isotopes are available [8–13]. This provides a good opportunity for a systematic study of the two-neutron removal from neutron-rich carbon isotopes. Simpson and Tostevin [7] have carried out a systematic theoretical analysis of the two-neutron removal from neutron-rich carbon isotopes using an eikonal reaction model in conjunction with shell model calculations. The calculations show that the one-neutron knockout plus neutron emission mechanism dominates over the direct two-nucleon removal mechanism. The theoretical calculations predict an odd-even mass staggering of two-neutron removal cross sections for  $^{15-20}\text{C}$ . These theoretically predicted trends are in good agreement with most of the experimental data, indicating the effectiveness of the eikonal reaction formalism

plus shell model in description of the two weakly bound neutron removal process.

However, it is found that the measured  $^{15}\text{C}$  two-neutron removal cross section data point [12] is significantly larger than the theoretical prediction [7] and does not follow the systematics of other experimental data.  $^{15}\text{C}$  is a one-neutron halo nucleus with small one-neutron separation energy of  $S_n = 1.218$  MeV. The special structure of  $^{15}\text{C}$  might offer the possibility that the reaction model combined with shell model calculations could not reproduce the measured two-neutron removal cross section. On the other hand, the experimentally measured cross section for  $^{15}\text{C}$  [12] also has relatively large uncertainty. Therefore, to resolve the discrepancy between the measured and calculated two-neutron removal cross sections from  $^{15}\text{C}$ , more measurements with better precision would be of value.

In this article we report a new measurement of the two-neutron removal cross sections from  $^{15,16}\text{C}$  secondary beams at around 240 MeV/nucleon and compare the theoretical predictions with the presently measured and the previously reported two-neutron removal cross sections from neutron-rich carbon isotopes.

**II. EXPERIMENT AND RESULTS**

The experiments were performed at the Heavy Ion Research Facility in Lanzhou (HIRFL) [14–16]. A primary beam of  $^{18}\text{O}$  was accelerated to 280 MeV/nucleon by the main Cooler Storage Ring (CSRm) [14]. The  $^{18}\text{O}$  beam was extracted from the CSRm and directed onto a beryllium target of 15 mm thickness. The reaction products from projectile fragmentation of  $^{18}\text{O}$  were separated according to their

\*wangshitao@impcas.ac.cn

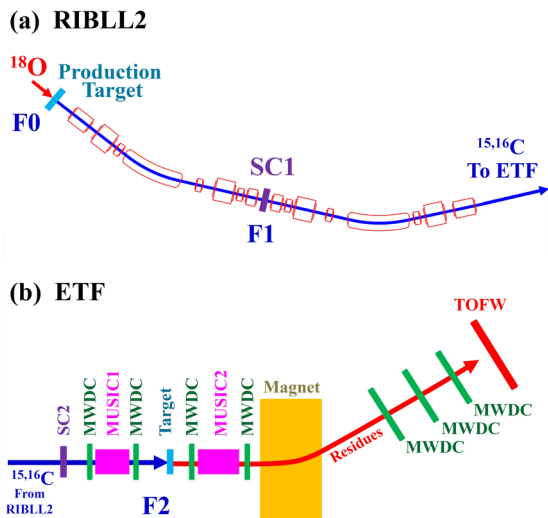


FIG. 1. Schematic view of the layout of (a) RIBLL2 and (b) ETF.

magnetic rigidity using the in-flight fragment separator RIBLL2 [15,17], the layout of which is shown in Fig. 1(a), and transported to the experimental site of the External Target Facility (ETF) [see Fig. 1(b)] [15]. The secondary beams were delivered as a cocktail beam containing different isotopes, and were identified based on a combination of the time of flight  $\text{TOF}_{\text{SC1} \rightarrow \text{SC2}}$  measured between two plastic scintillator detectors (denoted by SC1 and SC2 in Fig. 1) [18,19] and the energy loss  $\Delta E_{\text{MUSIC1}}$  measured with a multiple sampling ionization chamber (MUSIC1) located at the focal plane F2. Two magnetic rigidity settings for the RIBLL2 were used for producing  $^{15,16}\text{C}$  beams. The particle identification spectra for the cocktail beams are shown in Fig. 2, from which it can be seen that the various isotopes can be cleanly separated.

A 900-mg/cm<sup>2</sup>-thick carbon reaction target was mounted at the entrance of the ETF. The average mid-target energy of  $^{15,16}\text{C}$  was 237 and 239 MeV/nucleon, respectively. The trajectories of the incoming and outgoing particles before and after the target were measured by using four multiwire drift chambers (MWDCs), two before and two behind the target. In data analysis, the beam size on the target was limited to 4 cm in diameter by setting a software gate using the information from the MWDCs.

The reaction products as well as the unreacted beam particles were identified using the detector system of the ETF event by event by combining magnetic rigidity ( $B\rho$ ), time of flight (TOF), and energy loss ( $\Delta E$ ). The outgoing charged particles were deflected by a dipole magnet and bent at different angles inside the magnet depending on their charge to momentum ratios. The particle trajectories after the magnet were determined from the positions measured using three large area MWDCs behind the magnet, each having an active area of  $80 \times 60 \text{ cm}^2$ . The time of flight  $\text{TOF}_{\text{SC2} \rightarrow \text{TOFW}}$  was measured between a plastic scintillator (SC2) and a plastic scintillator wall (TOFW) with 30 strips and an active area of  $120 \times 120 \text{ cm}^2$  placed about 10 m downstream from the target. The time of flight was calibrated using the  $^{18}\text{O}$  primary beam, and a resolution of about 300 ps [full width at half max-

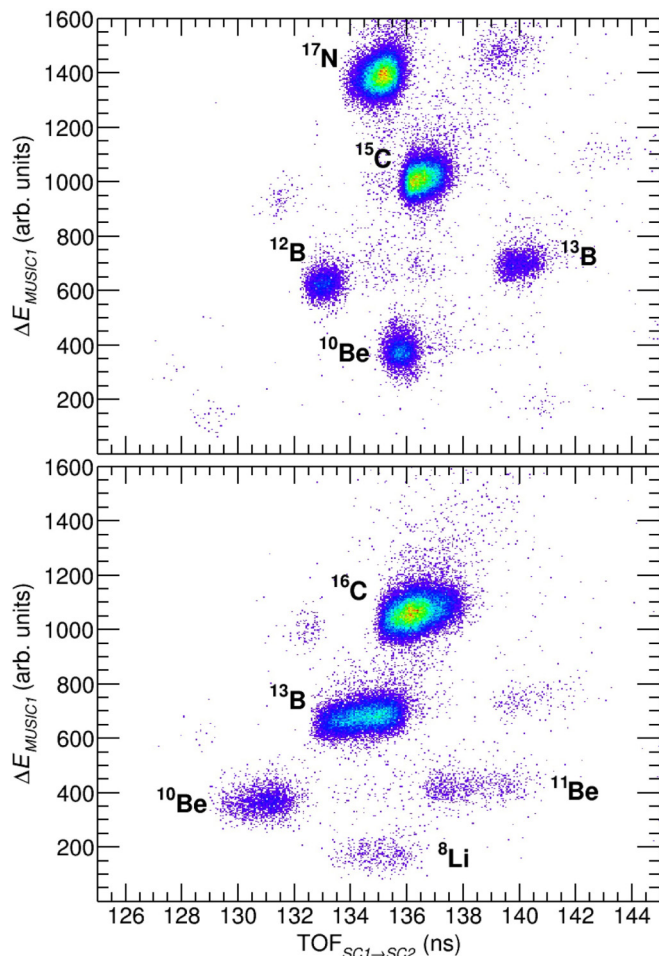


FIG. 2. The particle identification spectra for the incoming (a)  $^{15}\text{C}$  and (b)  $^{16}\text{C}$  beams.

imum (FWHM)] without any corrections was obtained. The energy loss  $\Delta E_{\text{MUSIC2}}$  was measured by a multiple sampling ionization chamber (MUSIC2) placed 50 cm downstream of the reaction target. The charge number  $Z$  of the reaction residues were identified by using the energy loss information. The fragment mass number  $A$  was deduced by applying the relation  $B\rho \sim (A/Z)\beta\gamma$ , where  $\beta$  and  $\gamma$  denote the velocity  $v/c$  and the relativistic Lorentz factor, respectively. A mass resolution of  $\sim 0.3$  mass units (FWHM), as shown in Fig. 3, was obtained. With such a resolution the mass  $A-2$  residues can be clearly separated from the intense unreacted mass  $A$  beam particles.

In the present experimental setting, the ETF provides a longitudinal momentum acceptance of 18% and a transverse momentum acceptance of 6%. The detection efficiency of the ETF detector system was calibrated using the secondary cocktail beams, and the obtained efficiencies were between 80% and 90%, depending on the charge number of the particles. The derived cross sections for ( $^{15}\text{C}$ ,  $^{13}\text{C}$ ) and ( $^{16}\text{C}$ ,  $^{14}\text{C}$ ) were  $\sigma_{-2n}(^{15}\text{C} \rightarrow ^{13}\text{C}) = 64(10) \text{ mb}$  and  $\sigma_{-2n}(^{16}\text{C} \rightarrow ^{14}\text{C}) = 97(13) \text{ mb}$ , respectively. The background contributions were measured by using target-out runs and subtracted. The total uncertainty in the cross sections mainly comes from

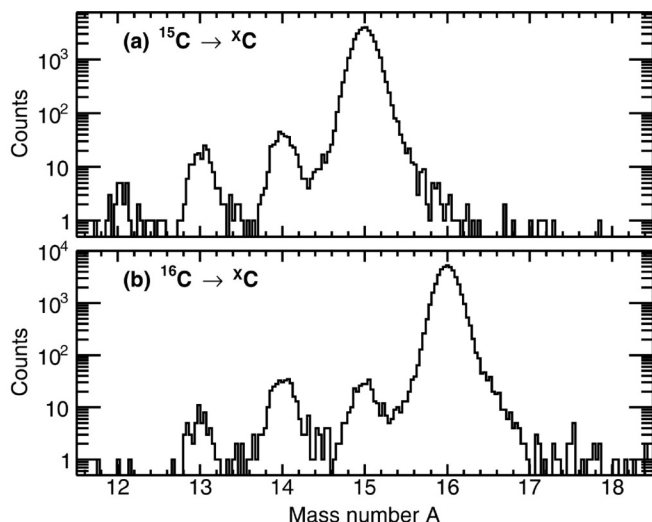


FIG. 3. The mass number  $A$  identification spectra of the particles after the reaction target for (a)  $^{15}\text{C}$  and (b)  $^{16}\text{C}$  incident beams. The particles are already charge selected for  $Z = 6$ .

statistical error. The uncertainty arising from the software gates used for particle identification and the transmission efficiency is estimated to be 5%.

### III. DISCUSSION

The experimental and calculated two-neutron removal cross sections across the carbon isotopic chain are summarized in Fig. 4. The measured cross sections from the present work for  $^{15,16}\text{C}$  at 240 MeV/nucleon on a carbon target are shown by red solid squares. The previously measured cross sections by other work for  $^{15-20}\text{C}$  [8–13] are shown by solid

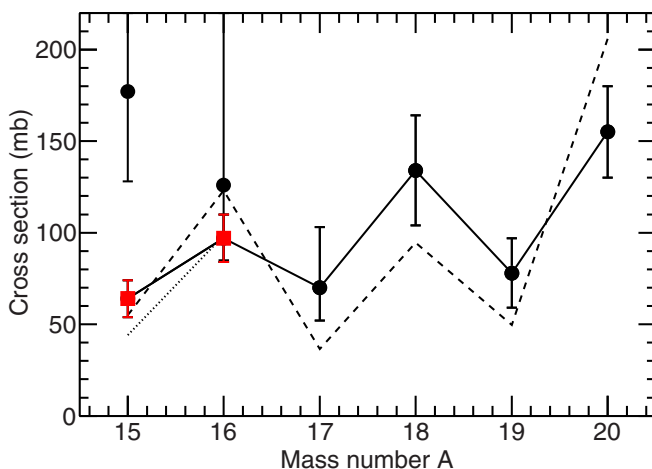


FIG. 4. Measured and calculated two-neutron removal cross sections for carbon isotopes. The solid line joins the measured cross sections of the present work for  $^{15,16}\text{C}$  (red solid squares) and other work for  $^{17-20}\text{C}$  (black solid circles) [8–11]. The measured cross sections for  $^{15,16}\text{C}$  in Refs. [12,13] are also shown by solid circles. The dashed line joins the calculated results from Refs. [7,8]. The dotted line connects the calculated results for  $^{15,16}\text{C}$  at 240 MeV/nucleon.

circles. These previous measurements are for a carbon target for the  $^{15}\text{C}$  [12],  $^{16}\text{C}$  [13],  $^{17}\text{C}$  [9],  $^{18}\text{C}$  [10], and  $^{20}\text{C}$  [8] projectiles, at 83, 83, 79, 80 and 240 MeV/nucleon, respectively, and for a beryllium target for  $^{19}\text{C}$  [11] at 64 MeV/nucleon. The measured cross sections from the present work for  $^{15,16}\text{C}$  and from other work for  $^{17-20}\text{C}$  [8–11] are joined by a solid line. The calculated cross sections for  $^{15-20}\text{C}$  at the same beam energies as the previous measurements are taken from Refs. [7,8] and are connected by a dashed line.

The theoretical two-neutron removal cross sections from  $^{15,16}\text{C}$  at 240 MeV/nucleon are estimated to be 44.04 and 98.43 mb, respectively, after multiplying the cross sections calculated at 83 MeV/nucleon [7] by a scaling factor of 0.8. The scaled cross sections at 240 MeV/nucleon are deduced based on the eikonal model calculations by taking into account the energy dependence. The eikonal model calculations are performed by using the computer code MOMDIS [20]. In the calculations for cross sections arising from indirect process, the required level energies and spectroscopic factors of the intermediate  $A-1$  residues are taken from Ref. [7]. Following Ref. [7], a reduced radius parameter of  $r_0 = 1.25$  fm and a diffuseness of  $a_0 = 0.7$  fm are used.

The scaled two-neutron cross sections from  $^{15,16}\text{C}$  at 240 MeV/nucleon are shown in Fig. 4 and connected by a dotted line. As can be seen from Fig. 4, the scaled cross sections at 240 MeV/nucleon are smaller than the calculated results at 83 MeV/nucleon. This is in keeping with the expectation for energy dependence that the cross section decreases as the beam energy increases from several tens of MeV/nucleon to a few hundred MeV/nucleon [8,21]. As shown in Fig. 4, the theoretical two-neutron removal cross sections of  $^{15-20}\text{C}$  within the eikonal model show a pronounced odd-even mass staggering, with the cross section being enhanced appreciably for the even-mass isotopes [7,8]. The staggering of the cross sections is understood as arising from the staggering of the neutron separation energies. The enhancement for two-neutron removal from even-mass  $A$  isotopes is explained to originate from the low one-neutron separation energy of the one-neutron knockout  $A-1$  residues with odd mass. With a low neutron separation energy, the excited unbound states of the intermediate  $A-1$  residues will contribute significantly to two-neutron removal yield by neutron decay. The calculations [7,8] indicate that the two-neutron removal cross sections due to indirect two-neutron removal are several times to an order of magnitude larger than those for the direct pair knockout.

Inspection of the experimental results in Fig. 4 shows that the measured two-neutron removal cross section of  $^{16}\text{C}$  at around 240 MeV/nucleon on a carbon target in this work is smaller than the previously measured value at 83 MeV/nucleon on a carbon target [13]. This is in agreement with the expectation for energy dependence. In contrast, the cross section for  $^{15}\text{C}$  measured at 83 MeV/nucleon [12] is significantly larger than the measured value at 240 MeV/nucleon and the calculated results at both energies. As a consequence, the trend of the cross sections between  $^{15}\text{C}$  and  $^{16}\text{C}$  from the present measurements and the theoretical predictions are also quite different from those measured previously [12,13]. It should be noted that the measured cross sections for  $^{15,16}\text{C}$  at 83 MeV/nucleon [12,13] have relatively large error bars,

as shown in Fig. 4. The large uncertainty lying in the cross section of  $^{15}\text{C}$  at 83 MeV/nucleon may be the reason for the discrepancies between the measured and calculated results.

Based on the present measurements on  $^{15,16}\text{C}$  combined with the available experimental data on  $^{17-20}\text{C}$ , an odd-even staggering of the two-neutron removal cross sections along the neutron-rich carbon isotopic chain from  $^{15}\text{C}$  to  $^{20}\text{C}$  is clearly observed, as shown in Fig. 4. The trends of the experimental data are qualitatively well reproduced by the theoretical calculations, although the experimental data points could not be quantitatively accurately reproduced. We note that to precisely calculate the two-neutron removal cross sections, an accurate shell model spectroscopic strength information within the energy window between the one- and two-neutron separation energy is needed, which is challenging for shell model calculations. On the other hand, the error bars on the experimental data are also appreciable. Nevertheless, these uncertainties in theoretical calculations and experimental data do not affect the conclusion that the experimentally observed odd-even staggering of the two-neutron removal cross sections from  $^{15}\text{C}$  to  $^{20}\text{C}$  is well reproduced by the eikonal model.

#### IV. SUMMARY

In summary, two-neutron removal experiments from  $^{15,16}\text{C}$  on a carbon target at a high energy of around 240 MeV/nucleon have been performed at the ETF of the HIRFL. The cross sections for ( $^{15}\text{C}$ ,  $^{13}\text{C}$ ) and ( $^{16}\text{C}$ ,  $^{14}\text{C}$ ) have been measured with higher precision compared with the previous measurements. The trends of the measured cross sections between  $^{15}\text{C}$  and  $^{16}\text{C}$  of the present data are different from those obtained previously, but in line with the theoretical predictions. The presently measured two-neutron removal cross sections for  $^{15,16}\text{C}$  combined with the available experimental data on  $^{17-20}\text{C}$  show a pronounced odd-even staggering, which is well reproduced by the theoretical calculations based on eikonal-model calculations combined with shell-model structure information.

#### ACKNOWLEDGMENT

This work was supported by the National Natural Science Foundation of China (Grants No. 11575257, No. U1732134, and No. 11305222).

- 
- [1] P. G. Hansen and J. A. Tostevin, *Annu. Rev. Nucl. Part. Sci.* **53**, 219 (2003).
- [2] B. A. Brown, P. G. Hansen, B. M. Sherrill, and J. A. Tostevin, *Phys. Rev. C* **65**, 061601(R) (2002).
- [3] D. Bazin, B. A. Brown, C. M. Campbell, J. A. Church, D. C. Dinca, J. Enders, A. Gade, T. Glasmacher, P. G. Hansen, W. F. Mueller, H. Olliver, B. C. Perry, B. M. Sherrill, J. R. Terry, and J. A. Tostevin, *Phys. Rev. Lett.* **91**, 012501 (2003).
- [4] J. A. Tostevin, G. Podolyak, B. A. Brown, and P. G. Hansen, *Phys. Rev. C* **70**, 064602 (2004).
- [5] K. Yoneda, A. Obertelli, A. Gade, D. Bazin, B. A. Brown, C. M. Campbell, J. M. Cook, P. D. Cottle, A. D. Davies, D.-C. Dinca, T. Glasmacher, P. G. Hansen, T. Hoagland, K. W. Kemper, J.-L. Lecouey, W. F. Mueller, R. R. Reynolds, B. T. Roeder, J. R. Terry, J. A. Tostevin, and H. Zwahlen, *Phys. Rev. C* **74**, 021303(R) (2006).
- [6] J. A. Tostevin and B. A. Brown, *Phys. Rev. C* **74**, 064604 (2006).
- [7] E. C. Simpson and J. A. Tostevin, *Phys. Rev. C* **79**, 024616 (2009).
- [8] N. Kobayashi, T. Nakamura, J. A. Tostevin, Y. Kondo, N. Aoi, H. Baba, S. Deguchi, J. Gibelin, M. Ishihara, Y. Kawada, T. Kubo, T. Motobayashi, T. Ohnishi, N. A. Orr, H. Otsu, H. Sakurai, Y. Satou, E. C. Simpson, T. Sumikama, H. Takeda *et al.*, *Phys. Rev. C* **86**, 054604 (2012).
- [9] C. Wu, Y. Yamaguchi, A. Ozawa, I. Tanihata, D. Jiang, H. Hua, T. Zheng, Z. Li, and Y. Ye, *J. Phys. G* **31**, 39 (2005).
- [10] A. Ozawa, D. Q. Fang, M. Fukuda, N. Iwasa, T. Izumikawa, H. Jeppesen, R. Kanungo, R. Koyama, T. Ohnishi, T. Ohtsubo, W. Shinozaki, T. Suda, T. Suzuki, M. Takahashi, I. Tanihata, C. Wu, and Y. Yamaguchi, *Phys. Rev. C* **78**, 054313 (2008).
- [11] M. Chiba *et al.*, *Nucl. Phys. A* **741**, 29 (2004).
- [12] D. Q. Fang, T. Yamaguchi, T. Zheng, A. Ozawa, M. Chiba, R. Kanungo, T. Kato, K. Morimoto, T. Ohnishi, T. Suda, Y. Yamaguchi, A. Yoshida, K. Yoshida, and I. Tanihata, *Phys. Rev. C* **69**, 034613 (2004).
- [13] T. Yamaguchi *et al.*, *Nucl. Phys. A* **724**, 3 (2003).
- [14] J. W. Xia *et al.*, *Nucl. Instrum. Methods Phys. Res. A* **488**, 11 (2002).
- [15] W. L. Zhan, H. S. Xu, G. Q. Xiao, J. W. Xia, H. W. Zhao, Y. J. Yuan, and HIRFL-CSR Group, *Nucl. Phys. A* **834**, 694c (2010).
- [16] W. L. Zhan *et al.*, *Nucl. Phys. A* **805**, 533c (2008).
- [17] Bao-Hua Sun *et al.*, *Sci. Bull.* **63**, 78 (2018).
- [18] Wen-Jian Lin *et al.*, *Chin. Phys. C* **41**, 066001 (2017).
- [19] J. W. Zhao *et al.*, *Nucl. Instrum. Methods Phys. Res. A* **823**, 41 (2016).
- [20] C. A. Bertulani and A. Gade, *Comput. Phys. Commun.* **175**, 372 (2006).
- [21] B. Blank *et al.*, *Nucl. Phys. A* **624**, 242 (1997).